Specific Interactions in 4-Hydroxybenzoic Acid/Poly(2-vinylpyridine)/Poly(*N*-vinyl-2-pyrrolidone) Blends

XUE-DONG LI, S. H. GOH

Department of Chemistry, National University of Singapore, 3 Science Drive 3, Singapore 117543

ABSTRACT: The specific interactions in ternary 4-hydroxybenzoic acid (HBA)/poly(2-vinylpyridine) (P2VPy)/poly(*N*-vinyl-2-pyrrolidone) (PVP) blends were studied by differential scanning calorimetry, Fourier transform infrared (FTIR) spectroscopy, and electron microscopy. FTIR study shows the existence of hydrogen-bonding interactions between HBA and P2VPy as well as PVP. The addition of a sufficiently large amount of HBA produces a blend showing one glass-transition temperature (T_g). Microscopic study shows a drastic reduction in domain size in single-T_g blends. © 2001 John Wiley & Sons, Inc. J Appl Polym Sci 81: 901–907, 2001

Key words: compatibilization; polymer blends; hydrogen-bonding interaction

INTRODUCTION

Two dissimilar polymers possessing complementary functional moieties are likely to be miscible with each other. For example, proton-accepting polymers such as poly(2-vinylpyridine) (P2VPy) and poly(*N*-vinyl-2-pyrrolidone) (PVP) are miscible with proton-donating polymers such as poly(*p*-vinylphenol)[1–4] and poly(methacrylic acid)[5–8] through hydrogen-bonding interactions. Therefore, one commonly used strategy to induce miscibility in an immiscible polymer blend is to incorporate suitable functional moieties onto one or both polymers.[9–15] Another strategy to achieve miscibility is to add a suitable polymer to an immiscible blend. A classic example is the addition of poly(vinylidene fluoride) (PVDF) to immiscible poly(methyl methacrylate) (PMMA)/poly-(ethyl methacrylate) (PEMA) blends.[16] Because PVDF is miscible with both PMMA and PEMA, the addition of a sufficient amount of PVDF can lead to a miscible ternary polymer blend.

Supramolecular polymeric materials based on polymer/low molecular weight compound systems have received increasing attention in recent years.[17–27] Specific interactions such as hydrogen-bonding and ionic interactions between a polymer and a low molecular weight compound can result in a material with new properties that neither component previously possessed. Particular attention has been directed to the formation of liquid crystalline polymers using the supramolecular approach.

Proton-accepting polymers such as P2VPy and PVP are generally immiscible with each other. However, a suitable bifunctional low molecular weight compound may offer some compatibilization effects if it can interact simultaneously with two different proton-accepting polymers. It is therefore of interest to study specific interactions in a ternary low molecular weight compound/polymer/polymer blend system. He et al.[28] recently reported a study on specific interactions between poly(ϵ-caprolactone) (PCL) with several bifunctional low molecular weight compounds. Thiodiphenol (TDP) was found to interact with PCL by hydrogen-bonding interaction. We now report our study on specific interactions in 4-hydroxybenzoic acid (HBA)/P2VPy/PVP blends. It is envisaged that the hydroxyl and carboxyl groups of HBA could interact with the two proton-accepting polymers, thus providing some compatibilization effects.

EXPERIMENTAL

Materials

P2VPy [weight-average molecular weight (M_w) = 200,000], was supplied by Scientific Polymer Products (Ontario, NY). PVP (M_w = 40,000) and HBA were supplied by Aldrich Chemical Company (Milwaukee, WI). All materials were used as received.

Preparation of Blends

P2VPy, PVP, and HBA were separately dissolved in ethanol (2% w/v). Binary P2VPy/HBA and PVP/HBA blends were prepared by mixing appropriate amounts of the ethanol solutions. Ternary blends of HBA, P2VPy, and PVP were prepared as follows. The ethanol solutions of HBA and P2VPy were mixed first. An appropriate amount of PVP solution was then added. In all cases the molar ratio of the repeating units of P2VPy to PVP was kept at 1 : 1, and only the ratio of the polymer to HBA was changed. The blends were denoted as polymer(HBA)$_x$, where x denotes the molar ratio of the repeating units of polymers to HBA. All the solution mixtures were clear and were continuously stirred for 48 h. The solvent was subsequently evaporated at room temperature to obtain solid blends. The blends were further dried *in vacuo* at 60°C for 2 weeks.

T_g Measurements

Glass-transition temperature (T_g) measurements were made on a TA Instruments 2920 differential scanning calorimeter (DSC; New Castle, DE). The blends were heated to 180°C at a heating rate of 20°C/min. The samples were kept at 180°C for 3 min before being quenched to −20°C. The quenched samples were then rescanned and the midpoints of the transition regions in the DSC curves were taken to be the T_g's. All measurements were conducted under a nitrogen atmosphere.

FTIR Characterization

FTIR spectra were recorded on a Bio-Rad 165 FTIR spectrophotometer (Bio-Rad, Richmond, CA); 32 scans were signal-averaged at a resolution of 2 cm^{-1}. In view of the hygroscopic nature of the polymers, spectra were recorded at 120°C, using a SPECAC high-temperature cell, equipped with an automatic temperature controller, which was mounted in the spectrophotometer. Blend samples were prepared by dropping the ethanol solutions to KBr powder followed by drying *in vacuo* at 60°C for 2 weeks. The mixtures were then ground and compressed to form disks. The KBr disks were further dried *in vacuo* at 60°C for another 2 days and then stored in a desiccator.

Optical Observation

The optical appearance of samples was examined using a Fisher-Johns melting point apparatus (Fisher Scientific, Pittsburgh, PA). A small amount of sample was sandwiched between two microscope cover glasses and heated in the melting-point apparatus until the sample softened and formed a film. The optical appearance of the film was observed with a magnifying glass attached to the apparatus.

Scanning Electron Microscopy

The films of samples were cryofractured in liquid nitrogen. The fracture surfaces were then sputter-coated with gold and observed with a Philips XL30 SEM (Philips, The Netherlands), using an accelerating voltage of 10–20 kV.

RESULTS AND DISCUSSION

Interaction Between Polymers and HBA

FTIR Characterization

Figure 1 shows the FTIR spectra in the carbonyl stretching regions of PVP, HBA, and various PVP(HBA)$_x$ blends. PVP shows a symmetrical
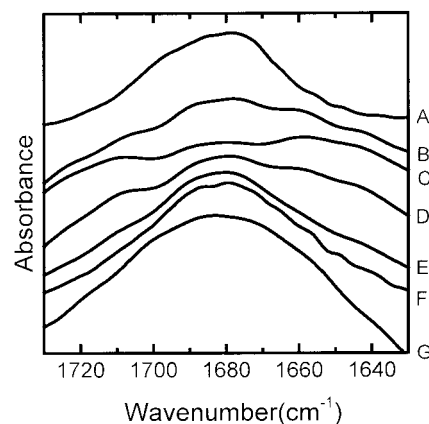

Figure 1 FTIR spectra, recorded at 120°C, in the carbonyl region of (A) HBA and various PVP(HBA)$_x$ blends: (B) $x = 1$; (C) $x = 2$; (D) $x = 4$; (E) $x = 10$; (F) $x = 20$; (G) PVP.
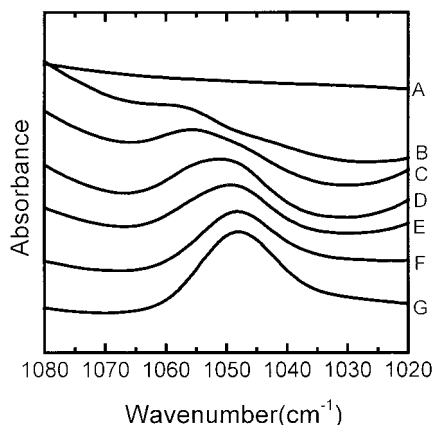
Figure 2 FTIR spectra, recorded at 120°C, in the pyridine region of (A) HBA and various P2VPy(HBA)$_x$ blends: (B) $x = 1$; (C) $x = 2$; (D) $x = 4$; (E) $x = 10$; (F) $x = 20$; (G) P2VPy.

Figure 4 DSC curves of PVP(HBA)$_x$ blends: (A) $x = 1$; (B) $x = 2$; (C) $x = 4$; (D) $x = 10$; (E) $x = 20$; (F) PVP.

carbonyl band at 1680 cm^{-1}. The carbonyl band of HBA is asymmetrical, consisting of a peak at 1675 cm^{-1} and a strong shoulder band at 1693 cm^{-1}. Carboxylic acids self-associate to form dimers. For HBA, self-association can proceed through hydroxyl–hydroxyl, hydroxyl–carboxyl, and carboxyl–carboxyl interactions. The latter two interactions are then responsible for the appearance of the asymmetrical carbonyl band of HBA. Although the carbonyl bands of PVP and HBA overlap, interaction between PVP and HBA is still evidenced from the spectra of the blends. It is known that a new carbonyl band develops at a lower frequency when the carbonyl groups of PVP undergo hydrogen-bonding interactions with proton-donating polymers.[29,30] A new band at 1654 cm^{-1} is observed in the PVP(HBA)$_x$ blends, show-
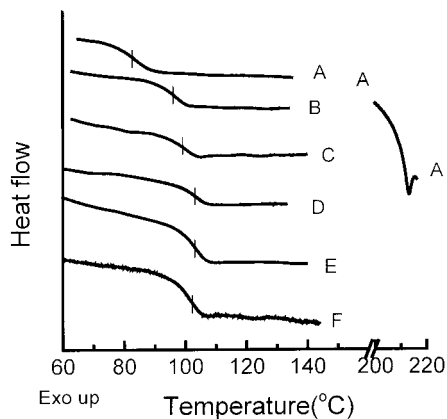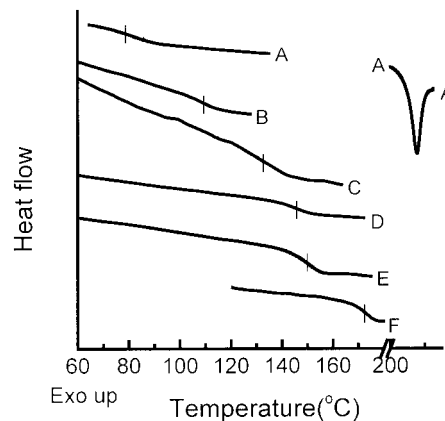
ing the existence of a hydrogen-bonding interaction between PVP and HBA. The blends also show the development of another new band at 1710 cm^{-1}. This band is ascribed to so-called free carbonyl groups when the self-association of HBA is disrupted by PVP–HBA interaction. He et al.[28] found that PCL interacts with TDP through hydrogen-bonding interaction as shown by the development of a new carbonyl band. However, PCL does not interact with 1,6-hexanediol (HDO).

For blends of P2VPy, the IR peaks at 1590 and 992 cm^{-1}, which arise from skeletal vibration of the pyridine ring, are most widely studied. However, these characteristic peaks are overlapped by the vibration of the phenyl ring of HBA. Nevertheless, the peak at 1050 cm^{-1} of P2VPy, the in-plane deformation of C—H in the pyridine ring, shifts to a higher frequency when the pyri-
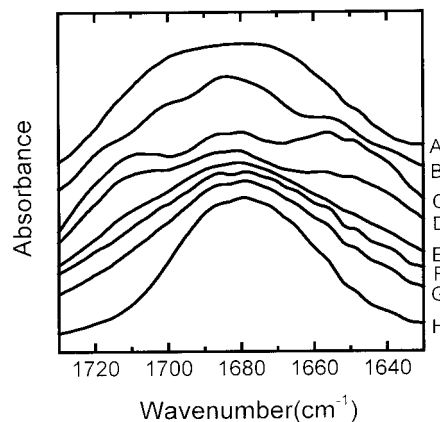

Figure 3 DSC curves of P2VPy(HBA)$_x$ blends: (A) $x = 1$; (B) $x = 2$; (C) $x = 4$; (D) $x = 10$; (E) $x = 20$; (F) P2VPy.

Figure 5 FTIR spectra, recorded at 120°C, in the carbonyl region of (A) HBA and various P2VPy–PVP(HBA)$_x$ blends: (B) $x = 1$; (C) $x = 2$; (D) $x = 4$; (E) $x = 8$; (F) $x = 20$; (G) $x = 40$; (H) P2VPy–PVP.

Figure 6 FTIR spectra, recorded at 120°C, in the pyridine region of (A) HBA and various P2VPy–PVP(HBA)$_x$ blends: (B) $x = 1$; (C) $x = 2$; (D) $x = 4$; (E) $x = 8$; (F) $x = 20$; (G) $x = 40$; (H) P2VPy–PVP.
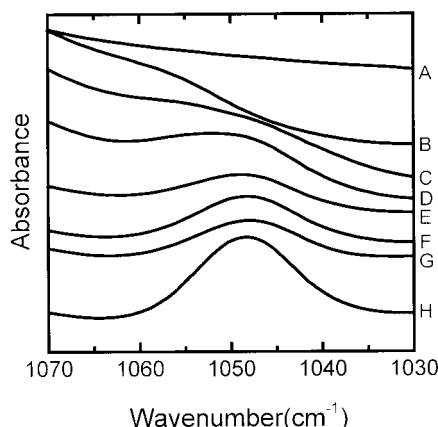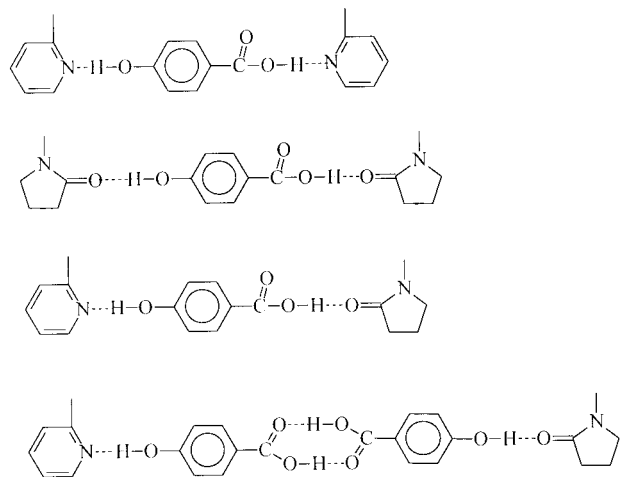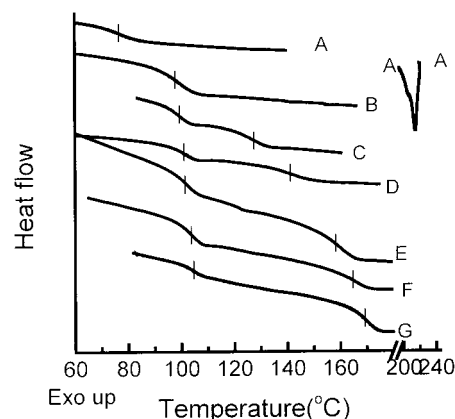

Figure 7 DSC curves of P2VPy–PVP(HBA)$_x$ blends: (A) $x = 1$; (B) $x = 2$; (C) $x = 4$; (D) $x = 8$; (E) $x = 20$; (F) $x = 40$; (G) P2VPy–PVP.

dine ring is involved in hydrogen-bonding interaction.[31] Figure 2 shows that this peak gradually shifts to a higher frequency upon the addition of HBA, confirming the existence of hydrogen-bonding interaction between P2VPy and HBA.

DSC Characterization

The influence of low molecular weight compounds on the T_g of polymers depends on the interaction strength between them. The small molecule acts as a plasticizer when the interaction is weak, and thus the T_g of polymer decreases upon the addition of small molecules. When the interaction between them is strong enough, as in some polyelec-

trolyte–surfactant systems, the T_g of polymer increases because the small molecules that interact with the polymer chains increase the rigidity of polymer chains and hinder chain motion.[32,33] In the present case, the addition of HBA lowers the T_g's of both P2VPy and PVP (Figs. 3 and 4). The DSC curves of P2VPy(HBA)$_1$ and PVP(HBA)$_1$ blends also show the melting peak of HBA, confirming the presence of HBA aggregates in the blends. It is of interest to note that the T_g of PCL increases upon the addition of TDP,[28] showing a stiffening effect. However, the T_g of PCL remains unchanged upon the addition of HDO.[28]

Compatibilization Effect of HBA on P2VPy/PVP Blends

FTIR Characterization

As mentioned earlier, the vibration regions of IR spectra between 1750 and about 1630 cm^{-1} [for

Scheme 1 Schematic diagram of various types of hydrogen-bonding interactions in P2VPy–PVP(HBA) ternary blends.
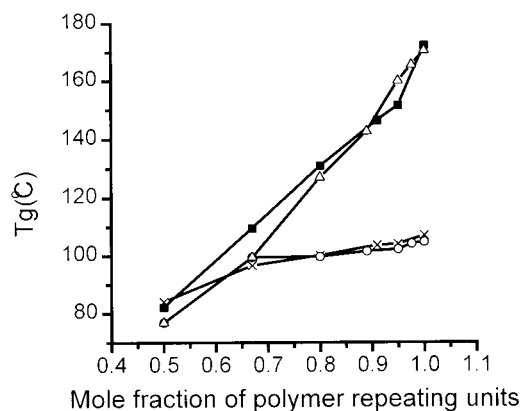

Figure 8 T_g's of various blends: (■) PVP/HBA; (×) P2VPy(HBA)$_x$; (△) PVP-P2VPy(HBA)$_x$ (high-T_g part); (○) PVP-P2VPy(HBA)$_x$ (low-T_g part).
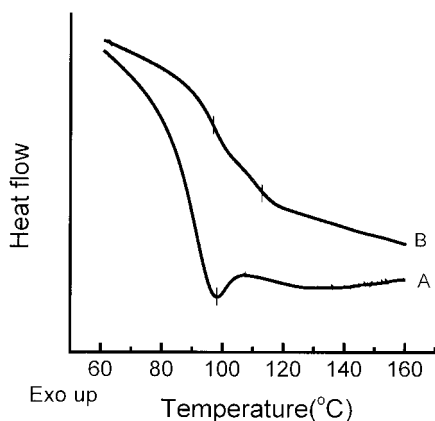
Figure 9   DSC curves of blends: (A) annealed P2VPy–PVP(HBA)$_2$ blend; (B) physical mixture of P2VPy(HBA)$_2$ and PVP(HBA)$_2$.

PVP(HBA)$_x$ blends], and between 1070 and about 1020 cm^{-1} [for P2VPy(HBA)$_x$ blends] show changes upon the formation of hydrogen bonding between HBA and the polymers. In the IR spectra of P2VPy–PVP(HBA)$_x$ ternary blends, similar changes in the two regions are also observed

(Figs. 5 and 6). Therefore both P2VPy and PVP interact with HBA in the ternary blends. There are various types of hydrogen-bonding interactions in the ternary blends, some of which are depicted in **Scheme 1**.

DSC Characterization

Figure 7 shows the DSC curves of ternary P2VPy–PVP(HBA)$_x$ blends. The binary polymer blend has two T_g's in the absence of HBA, indicating the immiscibility of the two polymers. The addition of increasing amounts of HBA (decreasing x value) depresses the T_g of PVP significantly, whereas the T_g of P2VPy is depressed slightly (Fig. 7). Only one T_g is observed for P2VPy–PVP(HBA)$_1$ and P2VPy–PVP(HBA)$_2$ blends. Moreover, the melting endotherm of HBA can be observed in the P2VPy–PVP(HBA)$_1$ blend. As shown in Figure 8, the two T_g values in the ternary blend are close to those of the binary P2VPy(HBA) and PVP(HBA) blends of the same composition. It then appears that the ternary blend consists of two plasticized polymer phases. However, when the HBA content is sufficiently
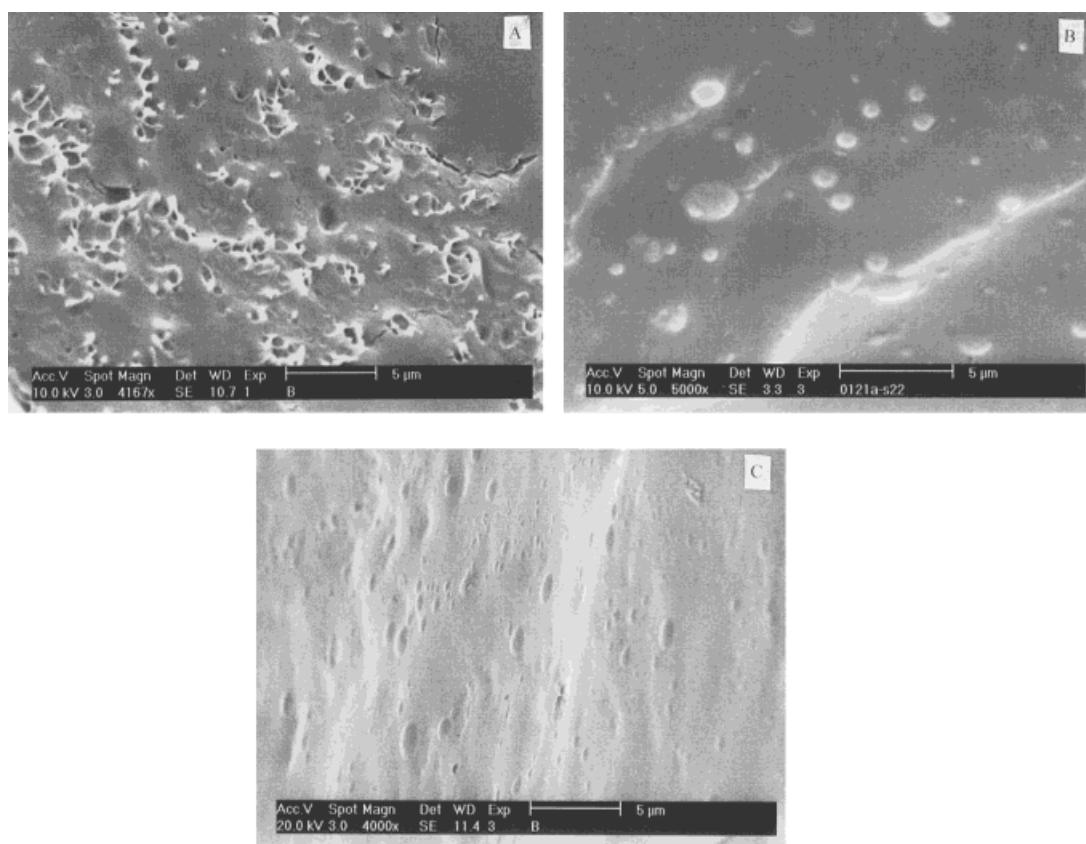

Figure 10   SEM micrographs of P2VPy–PVP(HBA)$_x$ blends: (A) P2VPy–PVP without HBA; (B) $x = 20$; (C) $x = 4$.

high, as in the P2VPy–PVP(HBA)$_2$ blend, the ternary blend shows a single T_g, whose value is intermediate to those of the binary P2VPy(HBA)$_2$ and PVP(HBA)$_2$ blends. The P2VPy–PVP(HBA)$_1$ blend also shows a single T_g. A two-phase polymer blend may show a single T_g, if the T_g values of the two phases are quite close to each other. In this type of situation, the blend is thermally annealed. An annealed two-phase blend shows two enthalpy relaxation peaks.[34] To establish whether the P2VPy–PVP(HBA)$_2$ blend consists of two phases with close T_g values, the blend was annealed at 60°C for 360 h. A physical mixture of P2VPy(HBA)$_2$ and PVP(HBA)$_2$ was also prepared. The annealed P2VPy–PVP(HBA)$_2$ blend shows one T_g, whereas the physical mixture shows two T_g's (Fig. 9). The DSC results show that the P2VPy–PVP(HBA)$_2$ blend is miscible, based on the single-T_g criterion. Therefore, the addition of a sufficiently large amount of HBA leads to the formation of a homogeneous blend. The homogeneity of the P2VPy–PVP(HBA)$_1$ blend is also shown by its optical clarity when heated above the melting temperature of HBA. In contrast, those blends with two T_g's are invariably cloudy.

SEM Observation

Figure 10 shows the morphology of P2VPy–PVP (1 : 1) blend in the absence of HBA. The two-phase nature of the immiscible blend is clearly evidenced. Because of the poor interfacial adhesion, some of the dispersed particles became detached from the fractured surface. Phase separation is still evident for the two-T_g P2VPy–PVP(HBA)$_{20}$ and P2VPy–PVP(HBA)$_4$ blends. However, the single-T_g P2VPy–PVP(HBA)$_2$ blend appears homogeneous under the same magnification [Fig. 11(A)]. At a higher magnification, uniform particles of about 30 nm in diameter can be seen in the blend [Fig. 11(B)].

CONCLUSIONS

In principle, a compatibilization effect is achieved when the two functional moieties of HBA interact with different types of polymers. However, most of the P2VPy–PVP(HBA)$_x$ blends possess two T_g's, indicating that the blends are phase separated; electron microscopy also confirms phase separation. Only when the x value is 1 or 2 does the blend show a single T_g. In other words, most of the HBA molecules interact with only one type
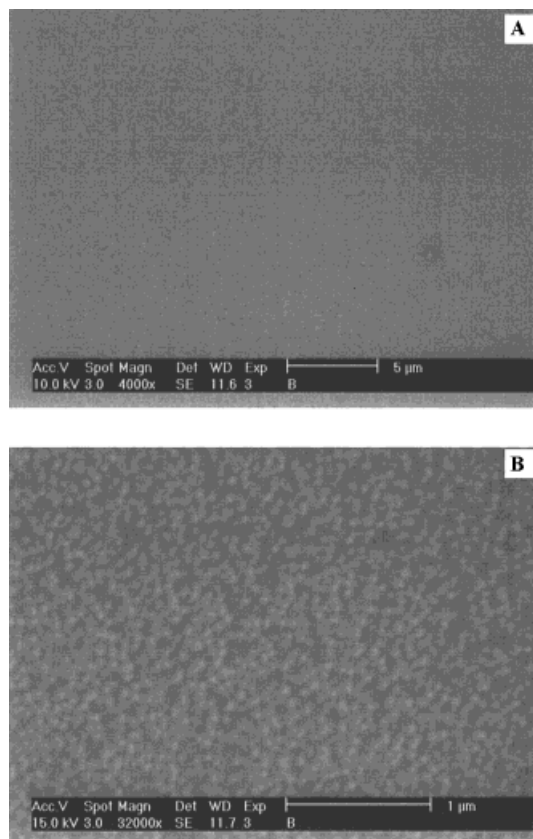

Figure 11 SEM micrographs of P2VPy–PVP(HBA)$_2$ blends: (A) ×4000; (B) ×32,000.

of polymer, resulting in a plasticizing effect. When the amount of HBA is large, the number of HBA interacting with two different types of polymers becomes sufficiently large to achieve a compatibilization effect. The domain size is then drastically reduced such that it cannot be detected by DSC. The large amount of HBA required to achieve the compatibilization effect implies that HBA is not an efficient compatibilizer. This may be the result of the close proximity of the two functional moieties in HBA, which makes it difficult to interact with two different types of polymer molecules. It is envisaged that an improvement in the compatibilization efficiency may be achieved if the two functional moieties are further separated by the introduction of some spacer groups.

REFERENCES

1. Wang, L. F.; Pearce, E. M.; Kwei, T. K. J Polym Sci Part B Polym Phys 1991, 29, 619.
2. Lee, J. Y.; Moskala, E. J.; Painter, P. C.; Coleman, M. M. Appl Spectrosc 1986, 40, 991.

3. Dai, J.; Goh, S. H.; Lee, S. Y.; Siow, K. S. Polym J 1994, 26, 905.

4. Zhou, X.; Goh, S. H.; Lee, S. Y.; Tan, K. L. Appl Surf Sci 1997, 60, 119.

5. Tsuchida, E.; Osada, Y.; Ohno, H. J Macromol Sci Phys 1980, B17, 683.

6. Smid, J.; Challa, G.; Tan, Y. Y. Polym Commun 1986, 27, 148.

7. Matuszewska–Czerwik, J.; Polowinski, S. Polym Bull 1988, 19, 149.

8. Zhou, X.; Goh, S. H.; Lee, S. Y.; Tan, K. L. Polymer 1998, 39, 3631.

9. Lu, S.; Pearce, E. M.; Kwei, T. K. Polymer 1995, 36, 2435.

10. Lu, S.; Pearce, E. M.; Kwei, T. K. Polym Adv Technol 1996, 7, 553.

11. Zhou, H.; Xiang, M.; Chen, W.; Jiang, M. Macromol Chem Phys 1997, 198, 809.

12. Zhu, L.; Jiang, M.; Liu, L.; Zhou, H.; Fan, L.; Zhang, Y.; Zhang, Y. B.; Wu, C. J Macromol Sci Phys 1998, B37, 805.

13. Zhu, L.; Jiang, M.; Liu, L.; Zhou, H.; Fan, L.; Zhang, Y. J Macromol Sci Phys 1998, B37, 827.

14. Goh, S. H.; Lau, W. W. Y; Lee, C. S. Polym Bull 1992, 29, 521.

15. Li, X.; Goh, S. H.; Lai, Y. H.; Wee, A. T. S. Polymer 2000, 41, 6563.

16. Kwei, T. K.; Frisch, H. L.; Radigan, W.; Vogel, S. Macromolecules 1977, 10, 157.

17. Lehn, J. M. Angew Chem Int Ed Engl 1990, 29, 1304.

18. Bazuin, C.G.; Tork, A. Macromolecules 1995, 28, 8877.

19. Bazuin, C. G. Mechanical and Thermophysical Properties of. Polymer Liquid Crystals; Chapman & Hall: London, 1998; Chapter 3.

20. Ruokolainen, J.; Makinen, P.; Torkkeli, M.; Makela, T.; Serimaa, R.; ten Brinke, G.; Ikkala, O. Science 1998, 280, 557.

21. Ruokolainen, J.; Tanner, J.; Ikkala, O.; ten Brinke, G.; Thomas, E. L. Macromolecules 1998, 31, 3532.

22. Kato, T.; Kirota, N.; Fujishima, A.; Frechet, J. M. J. J Polym Sci Part A Polym Chem 1996, 34, 57.

23. Kawakami, T.; Kato, T. Macromolecules 1998, 31, 4475.

24. Alder, K. I.; Stewart, D.; Imrie, C. T. J Mater Chem 1995, 5, 2225.

25. Stewart, D.; Paterson, B. J.; Imrie, C. T. Eur Polym J 1997, 33, 285.

26. Yan, H.; Zhu, X. J Appl Polym Sci 1999, 74, 97.

27. Lange, R. F. M.; Van Gurp, M.; Meijer, E. W. J Polym Sci Part A Polym Chem 1999, 37, 3657.

28. He, Y.; Asakawa, N.; Inoue, Y. J Polym Sci Part B Polym Phys 2000, 38, 1848.

29. Moskala, E. J.; Varnell, D. F.; Coleman, M. M. Polymer 1985, 26, 228.

30. Cesteros, L. C.; Meaurio, E.; Katime, I. Polym Int 1994, 34, 97.

31. Lee, J. Y.; Painter, P. C.; Coleman, M. M. Macromolecules 1988, 21, 954.

32. Hsiao, M. S.; Chen, H. L.; Liaw, D. J. Macromolecules 2000, 33, 221.

33. Chen, H. L.; Hsiao, M. S. Macromolecules 1999, 32, 2967.

34. ten Brinke, G.; Oudhuis, L.; Ellis, T. S. Thermochim Acta 1994, 238, 75.